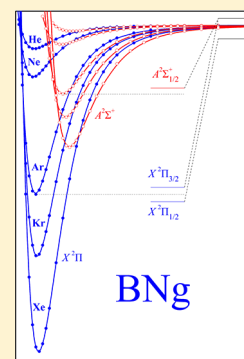


# Accurate ab Initio Structural Parameters of the Diatomic and Triatomic van der Waals Molecules $^{11}\text{BNg}$ ( $X^2\Pi$ , $A^2\Sigma^+$ ) and $^{11}\text{BNg}_2$ ( $\tilde{X}^2B_1$ ), Ng = $^4\text{He}$ , $^{20}\text{Ne}$ , $^{40}\text{Ar}$ , $^{84}\text{Kr}$ , and $^{132}\text{Xe}$

Ilias Magoulas, Aristotle Papakondylis, and Aristides Mavridis\*

Laboratory of Physical Chemistry, Department of Chemistry, National and Kapodistrian University of Athens, Panepistimiopolis, Athens 15771, Greece

**ABSTRACT:** The weakly interacting BNg and BNg<sub>2</sub> molecular systems, Ng = He, Ne, Ar, Kr, and Xe, have been thoroughly studied through coupled-cluster RCCSD(T) calculations and large correlation consistent basis sets. For the BNg diatomics, the states examined are the  $X^2\Pi$  and  $A^2\Sigma^+$ , and the  $\tilde{X}^2B_1$  state for the C<sub>2v</sub> BNg<sub>2</sub> triatomics. A series of corrections render our final results reliable, judging as well from the (limited) experimental numbers available. Both BHe and BHe<sub>2</sub> are marginally unbound, whereas the attractive interactions of the BNg  $X^2\Pi$  states, where Ng = Ne, Ar, Kr, and Xe, are  $D_0 = 19.8, 98.2, 141.9,$  and  $209.1 \text{ cm}^{-1}$ , respectively. For the BRn (Rn = radon) species, an estimated value of interaction energy  $D_0 \approx 280 \text{ cm}^{-1}$  is obtained by a  $D_0$  versus static polarizability ( $\alpha$ ) extrapolation. Corresponding atomization energies of the BNg<sub>2</sub> ( $\tilde{X}^2B_1$ ) molecules are  $AE_0 = 52.0$  (BNe<sub>2</sub>), 263.4 (BAr<sub>2</sub>), 384.6 (BKr<sub>2</sub>), and 576.9 (BXe<sub>2</sub>)  $\text{cm}^{-1}$ .



## 1. INTRODUCTION

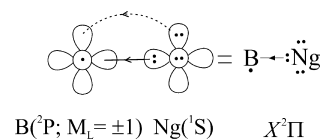
Not so many years ago, we have published a series of very accurate theoretical papers on the electronic structure of the  $X^2\Sigma^+$ ,  $A^2\Pi$ , and  $B^2\Sigma^+$  states of the lithium-noble gas diatomics, LiNg, where Ng = He, Ne, Ar, and Kr.<sup>1–3</sup> With respect to the first excited state of Li\* ( $^2P; 1s^2 2p^1$ ), 1.848 eV above the ground  $^2S$  state,<sup>4</sup> the calculated binding energies of the  $A^2\Pi$  states of the LiNg species are  $D_0 = D_e - (\omega_e/2) + (\omega_e x_e/4) = 842.6,$ <sup>1</sup> 164.8,<sup>2</sup> 794.6,<sup>3</sup> and 1129.0<sup>3</sup>  $\text{cm}^{-1}$  for Ng = He, Ne, Ar, and Kr, respectively. Recall that the  $^2P(2p^1)$  state of the Li atom is “isovalent” to the ground  $^2P(2s^2 2p^1)$  state of the B atom. Therefore, the Boron–Ng interactions are expected to be of similar nature to those of Li\*( $^2P$ )–Ng, albeit, considerably smaller as compared to the  $A^2\Pi$  state of the latter.

The present work is a highly accurate systematic study of the  $X^2\Pi$  and  $A^2\Sigma^+$  states of the  $^{11}\text{BNg}$  diatomics, Ng =  $^4\text{He}$ ,  $^{20}\text{Ne}$ ,  $^{40}\text{Ar}$ ,  $^{84}\text{Kr}$ , and  $^{132}\text{Xe}$  through single reference coupled-cluster calculations [RCCSD(T)], extended correlation consistent basis sets, and complemented by a series of corrections some of them mandatory if we are after quantitative results. The essence of the B( $^2P$ )–Ng “bonding” interaction is captured by the valence bond–Lewis (vbL) Schemes (1) and (2), clearly showing the cause of the expected weak van der Waals type interactions, taking into account as well the nature of the Ng atoms.

The BHe system obviously lacks  $\pi_p$  electrons which can be of some assistance to the van der Waals (vdW) interaction.

We have also examined at the coupled-cluster (CC) level the triatomics BNg<sub>2</sub> ( $\tilde{X}^2B_1$ ), whose geometries and bonding can also be understood by inspecting the vbL diagram (1), but see below. Notice that, in essence, no experimental or theoretical results are available on BNg<sub>2</sub> complexes.

### Scheme 1



### Scheme 2

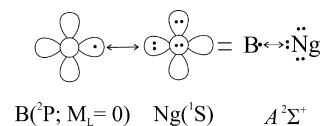


Table 1 presents all experimental and theoretical structural results on the BNg systems available in the literature concerning the  $X^2\Pi$  and  $A^2\Sigma^+$  states. It is worth noting the following: experimental results are scarce, limited to three dissociation energies (BNe,<sup>5</sup> BAr,<sup>6</sup> BKr<sup>8</sup>) and one bond distance for the  $X^2\Pi_{1/2}$  state of BAr.<sup>7</sup> Theoretical predictions are also very limited, confined mostly to  $D_e$  and  $r_e$  for both  $X^2\Pi$  and  $A^2\Sigma^+$  states, three  $D_0$  and one  $r_0$  (BAr) values (see Table 1). Most importantly, the type of published calculations is not high enough, thus rendering the numbers of Table 1 of questionable validity, particularly for this kind of system; see the explicatory footnotes of Table 1. Therefore, the need for a comprehensive, high quality ab initio study of these very weakly interacting systems seems in order.

Received: March 19, 2014

Revised: May 7, 2014

Published: May 7, 2014

**Table 1. Experimental and Theoretical Results on  $^{11}\text{BNg}$ ,  $\text{Ng} = \text{He, Ne, Ar, Kr, Xe}$ , from the Literature<sup>a</sup>**

state	species	$D_e$	$D_0$	$r_e$	$r_0$
		experiment			
$X^2\Pi_{1/2}$	$\text{BNe}^b$		$21.3 \pm 0.2$		
	$\text{BAr}$		$102.4 \pm 0.3^c$		$3.606 \pm 0.007^d$
	$\text{BKr}^e$		$159.4 \pm 1.2$		
		theory			
$X^2\Pi_{1/2}$	$\text{BNe}^f$		17.5		
$X^2\Pi$	$\text{BAr}^g$	94.7	75.1	3.671	3.703
	$\text{BAr}$	$109.7^h$	$106.1^f$	$3.62^h$	
	$\text{BKr}^h$	146.8		3.67	
	$\text{BXe}^h$	196.8		3.73	
$A^2\Sigma^+$	$\text{BAr}^g$	38.4		4.447	
	$\text{BAr}^h$	45.2		4.43	
	$\text{BKr}^h$	60.5		4.50	
	$\text{BXe}^h$	67.8		4.70	

<sup>a</sup>Equilibrium distances are  $r_e$  and  $r_0$  (Å), and dissociation energies are  $D_e$  and  $D_0$  ( $\text{cm}^{-1}$ ). <sup>b</sup>Ref 5. Laser Fluorescence Spectroscopy (LFS), under the assumption of barrierless dissociation to  $\text{B}(2s^1 2p^2; ^2D)$ . <sup>c</sup>Ref 6. LFS, under the assumption of barrierless dissociation. <sup>d</sup>Ref 7. LFS. <sup>e</sup>Ref 8. LFS; under the assumption of barrierless dissociation. <sup>f</sup>Ref 9. UCCSD(T)/aug-cc-pVQZ; after scaling ( $s = 1.25$ ),  $D_0 = 20.0 \text{ cm}^{-1}$ . <sup>g</sup>Ref 7. MRACPF/cc-pVQZ+spdfg diffuse functions. <sup>h</sup>Ref 10. UCCSD(T) /aug-cc-pVQZ/<sub>B</sub> ECP-Stuttgart/<sub>Ng</sub>. <sup>i</sup>Ref 11. After applying an ad hoc scaling factor,  $s = 1.19$ , to the  $D_0 = 75.1 \text{ cm}^{-1}$  (ref 7) also using the experimental  $D_0^0 = 102.4 \text{ cm}^{-1}$  from ref 6.

For all  $\text{BNg}$  ( $\text{Ng} = \text{He, Ne, Ar, Kr, and Xe}$ ) molecules, we report full potential energy curves (PEC), spectroscopic parameters, and permanent electric dipole moments. All our results for the  $X^2\Pi$  states have been corrected for basis set superposition errors (BSSE), spin-orbit splittings (SO), core

and scalar relativistic effects, and extrapolated to the complete basis set (CBS) limit. The  $\text{BNg}_2$  triatomics have been treated at a lower level, but certainly our predicted numbers are judged to be quite reliable.

The paper is organized as follows. Section 2 refers to the computational details, section 3 (3A, 3B, and 3C) to results and discussion, whereas the closing section 4 is a short summary of this work.

## 2. BASIS SETS AND METHODS

Through all calculations, the augmented valence correlation consistent (cc) generally contracted basis sets have been used, namely aug-cc-pVnZ ( $= \text{An}\zeta$ ), where  $n = \text{Q, 5, and 6}$  for both atoms B and Ng.<sup>12–14</sup> For the diatomics  $\text{BHe, BNe, and BAr}$  in particular, the  $\text{An}\zeta$  ( $n = \text{Q, 5, and 6}$ ) basis sets have been employed, while for  $\text{BKr}$ , the  $\text{AS}\zeta$  basis was used ( $\text{AS}\zeta_{\text{B}}/\text{AS}\zeta_{\text{Kr}}$ ). For the very heavy Xe ( $Z = 54$ ) atom, the inner 28 electrons ( $[\text{Ar}]3d^{10}$ ) were replaced by the relativistic effective core potentials of Peterson et al.,<sup>15</sup> hereafter denoted as PP. The remaining 26 electrons are represented by the appropriate cc  $\text{AS}\zeta$  basis set;<sup>15</sup> hence, the basis set of the  $\text{BXe}$  molecule can be written as  $\text{AS}\zeta_{\text{B}}/\text{AS}\zeta_{\text{Xe}}\text{-PP}/\text{Xe} (= \text{AS}\zeta\text{-PP})$ .

As to the first four triatomics,  $\text{BNg}_2$  ( $\text{Ng} = \text{He–Kr}$ ) and  $\text{BXe}_2$ , the basis sets used are  $\text{AS}\zeta_{\text{B}}/\text{AS}\zeta_{\text{Ng}}$  and  $\text{AS}\zeta_{\text{B}}/\text{AS}\zeta_{\text{Xe}}\text{-PP}/\text{Xe}$ , respectively.

For all  $\text{BNg}$  ( $X^2\Pi, A^2\Sigma^+$ ) and  $\text{BNg}_2$  ( $\tilde{X}^2B_1$ ),  $\text{Ng} = \text{He–Xe}$ , the calculation approach followed is the single reference restricted coupled-cluster+singles+doubles+quasi-perturbative connected triples method,  $\text{RCCSD(T)}$ .<sup>16–18</sup> Constraints of the  $\text{C}_{2v}$  Abelian point group have been imposed through all calculations.

Core corrections for the first three diatomics,  $1s^2$  on B ( $\text{BHe}$ ),  $1s^2/1s^2$  ( $\text{BNe}$ ), and  $1s^2/2s^2 2p^6$  ( $\text{BAr}$ ), have been taken

**Table 2. Total Energies,  $E$  ( $E_h$ ), Bond Lengths,  $r_e$  and  $r_0$  (Å), Dissociation Energies,  $D_e$  and  $D_0$  ( $\text{cm}^{-1}$ ), Harmonic Frequencies,  $\omega_e$  ( $\text{cm}^{-1}$ ), and Anharmonic Corrections,  $\omega_e x_e$  ( $\text{cm}^{-1}$ ), Rotational Vibrational Coupling Constants,  $\alpha_e$  ( $\text{cm}^{-1}$ ), Dipole moments,  $\mu_e$  (D), Equilibrium BSSE/ $r_e$  values ( $\text{cm}^{-1}$ ), Separation Energies  $T$  ( $\text{cm}^{-1}$ ) of the  $X^2\Pi$  and  $A^2\Sigma^+$  States of the  $\text{BNg}$  Species, Where  $\text{Ng} = \text{He, Ne, Ar, Kr, Xe}$ , Calculated at the  $\text{RCCSD(T)}/\text{An}\zeta$  Level of Theory. BSSE is Dynamically Corrected**

$\text{BNg}/n$	$-E$	$r_e$	$r_0$	$D_e$	$D_0^a$	$\omega_e$	$\omega_e x_e$	$\alpha_e \times 10^2$	$\mu_e^b$	BSSE/ $r_e$	$T_e/T_0$
						$X^2\Pi$					
$\text{BHe}/5$	27.504 803	3.551	4.617	16.6	3.33	26.6			0.010	0.52	0.0
$\text{BHe}/6$	27.505 272	3.540	4.587	17.2	3.48	27.4			0.010	0.15	0.0
$\text{BHe}/\text{CBS}^c$		3.531	4.566	17.8	3.58						
$\text{BNe}/5$	153.461 55	3.520	3.808	36.5	21.9	28.8	6.0	3.9	0.022	5.17	0.0
$\text{BNe}/6$	153.465 95	3.506	3.793	37.8	22.8	29.6	6.1	3.8	0.022	1.98	0.0
$\text{BNe}/\text{CBS}^c$		3.495	3.779	39.2	23.6						
$\text{BAr}/5$	551.685 55	3.585	3.692	119.5	97.1	46.6	4.1	1.4	0.080	11.2	0.0
$\text{BAr}/6$	551.690 12	3.577	3.682	122.6	99.9	47.2	4.1	1.4	0.080	4.82	0.0
$\text{BAr}/\text{CBS}^c$		3.571	3.676	123.6	101.6						
$\text{BKr}/5$	2776.683 17	3.634	3.715	163.2	139.2	49.8	3.6	0.88	0.119	8.67	0.0
$\text{BKr}/\text{CBS}^d$		3.611	3.690	170.4	146.0						
$\text{BXe}/5\text{-PP}^e$	353.101 64	3.680	3.744	230.7	204.0	55.1	3.2	0.65	0.196	8.02	0.0
$\text{BXe}/\text{CBS}^f$		3.664	3.728	238.0	210.9						
						$A^2\Sigma^+$					
$\text{BHe}/6$	27.505 214	4.648		4.47						0.03	12.7
$\text{BNe}/6$	153.465 84	4.337	4.928	14.1	6.15	16.0		4.5		0.98	23.7/16.6
$\text{BAr}/6$	551.689 78	4.382	4.580	50.0	36.9	29.2	5.1	0.96		2.38	72.6/63.0
$\text{BKr}/5$	2776.882 70	4.468	4.611	64.9	51.4	28.2	2.8			4.19	98.3/87.8
$\text{BXe}/5\text{-PP}^e$	353.100 96	4.586	4.700	86.1	71.3	71.3	2.7	0.66		3.33	144.3/132.7

<sup>a</sup> $D_0 = D_e - \text{ZPE}$ . <sup>b</sup>Calculated through the finite field approach; field strengths =  $10^{-4}$  a.u. <sup>c</sup>Complete basis set limit obtained at the  $\text{RCCSD(T)}/\text{AQ}\zeta\text{-AS}\zeta\text{-A6}\zeta$  (Q56) level. <sup>d</sup>(TQ5) Douglas–Kroll–Hess limit. <sup>e</sup>Effective core potential on Xe; see text. <sup>f</sup>(TQ5)-PP CBS limit.

into account by using the aug-cc-pCV5Z basis sets,<sup>13,14</sup> while no core corrections were applied to BKr and of course to BXe. Scalar relativistic corrections on BNg (Ng = He–Kr) were considered via the eighth-order Douglas-Kroll-Hess (DKH) approximation<sup>19–21</sup> in conjunction with the aug-cc-pVnZ-DK basis sets recontracted accordingly.<sup>22</sup>

Spin–orbit (SO) splittings were calculated by diagonalizing the  $\hat{H}_e + \hat{H}_{SO}$  Hamiltonian within the valence internally contracted CASSCF+1+2 = MRCI/A6 $\zeta$  (BHe, BNe, BAr), MRCI/AS $\zeta$  (BKr), and MRCI/AS $\zeta$ -PP (BXe) eigenvectors of  $\hat{H}_j$ ;  $\hat{H}_{SO}$  stands for the full Breit–Pauli operator. The CASSCF wave functions are obtained by distributing 5e<sup>−</sup> to 5 orbitals for BHe (2s2p<sub>B</sub>+1s<sub>He</sub>) and 9 e<sup>−</sup> to 7 orbitals (2s2p<sub>B</sub>+np<sub>Ng</sub>) for the rest of the BNg (Ng = Ne–Xe) species. Notice that the MRCI calculations have been employed solely for obtaining the SO splittings.

BSSE corrections, undoubtedly of importance for vdW molecules, were calculated through the usual counterpoise approach and along the entire B–Ng coordinate (dynamical BSSE<sup>23–25</sup>).

CBS limits for selected properties of the X<sup>2</sup>Π state of BNg ( $r_e$ ,  $r_0$ ,  $D_e$ , and  $D_0$ ) have been estimated using the simple exponential

$$P_n = P_\infty + Ae^{-Bn}$$

and the mixed exponential-Gaussian

$$P_n = P_\infty + Ae^{-(n-1)} + Be^{-(n-1)^2}$$

formulas of Peterson and Dunning<sup>26</sup> and Peterson et al.,<sup>27</sup> respectively. In the formulas above  $P$  is a generic property,  $P_\infty$  its CBS limit,  $n$  is the cardinal number of the basis set, while  $A$  and  $B$  are fitting parameters. Our reported CBS limits are the arithmetic mean values of the above two relations.

Finally, the zero-point energy corrections (ZPE) and spectroscopic constants of the BNg diatomics were determined by numerically solving the radial Schrödinger equation for the B and Ng nuclei.

All calculations have been performed by MOLPRO2012.<sup>28</sup>

### 3. RESULTS AND DISCUSSION

Table 2 lists numerical results for both states (X<sup>2</sup>Π and A<sup>2</sup>Σ<sup>+</sup>) of the BNg (Ng = He–Xe) species. Notice that all values, but the total energies, have been corrected dynamically for BSSE. Table 3 refers to the SO interactions of the X<sup>2</sup>Π states and of the B atom calculated at the MRCI level, while Table 4 shows final results on the X<sup>2</sup>Π states of BNg after the imposition of SO, core, and scalar relativistic corrections. Core and relativistic

**Table 3. Calculated and Experimental Spin-Orbit Splittings  $\Delta T$  (cm<sup>−1</sup>) = <sup>2</sup>Π<sub>3/2</sub>–<sup>2</sup>Π<sub>1/2</sub> States of the BNg Molecules, Ng = He, Ne, Ar, Kr, and Xe and of the B Atom (<sup>2</sup>P<sub>3/2</sub>–<sup>2</sup>P<sub>1/2</sub>) at the MRCI Level Around Equilibrium**

species	basis set	$\Delta T^a$ calcd.	$\Delta T$ exptl.
BHe	A6 $\zeta$	10.15	
BNe	A6 $\zeta$	10.53	
BAr	A6 $\zeta$	10.32	10.88 ± 0.08 <sup>b</sup>
BKr	A5 $\zeta$	10.87	
BXe	AS $\zeta$ -PP <sup>c</sup>	15.35	
B	A6 $\zeta$	14.34	15.287 <sup>d</sup>

<sup>a</sup> $\Delta T = A\Lambda\Sigma$ , where  $A$  is the SO coupling constant. <sup>b</sup>Ref 29. <sup>c</sup>Effective core potentials. <sup>d</sup>Ref 4.

**Table 4. Final (CBS, SO, Core, and Relativistically Corrected) Bond Lengths,  $r_0$  (Å), and Dissociation Energies,  $D_0$  (cm<sup>−1</sup>), of the X<sup>2</sup>Π<sub>1/2,3/2</sub> States of BNg, Where Ng = He, Ne, Ar, Kr, and Xe<sup>a</sup>**

species <sup>b</sup>	$r_0$	$D_0(1/2-1/2)^c$	$D_0(3/2-3/2)^d$
BHe	4.568	−0.71	3.48
BNe	3.785	19.8 (21.3 ± 0.2) <sup>e</sup>	23.6
BAr	3.673 (3.606 ± 0.007) <sup>e</sup>	98.2 (102.4 ± 0.3) <sup>e</sup>	102.2
BKr	3.690	141.9 (159.4 ± 1.2) <sup>e</sup>	145.4
BXe	3.728	209.1	208.1

<sup>a</sup>Existing experimental values for easy comparison are in parentheses. <sup>b</sup>For details of obtaining the values above see the text. <sup>c</sup>BNg(X<sup>2</sup>Π<sub>1/2</sub>) → B(<sup>2</sup>P<sub>1/2</sub>)+Ng(<sup>1</sup>S). <sup>d</sup>BNg(X<sup>2</sup>Π<sub>3/2</sub>) → B(<sup>2</sup>P<sub>3/2</sub>)+Ng(<sup>1</sup>S). <sup>e</sup>See Table 1.

corrections combined are indeed small, changing the bond distances and dissociation energies by  $\delta r_0 = +0.0016, +0.0068, -0.0033$  Å and by  $\delta D_0 = -0.100, +0.23, +0.84$  cm<sup>−1</sup> for BHe, BNe, and BAr, respectively. Core corrections have not been applied to BKr and BXe, but only relativistic corrections through CBS TQ5-DKH (BKr) and TQ5-PP (BXe) limits. Final  $\omega_e$ ,  $\omega_e x_e$ ,  $a_e$ , and  $\mu_e$  constants of the X<sup>2</sup>Π state of BNg are those given in Table 2 at the RCCSD(T)/A6 $\zeta$  level (Ng = He, Ne, and Ar) and RCCSD(T)/AS $\zeta$ , AS $\zeta$ -PP for Kr and Xe, respectively.

Table 5 lists numerical results for the triatomics BNg<sub>2</sub> (Ng = He–Xe) calculated at the RCCSD(T)/AS $\zeta$  level. Notice that only equilibrium BSSE corrections have been applied to all the BNg<sub>2</sub> triatomics.

Figure 1 illustrates the X<sup>2</sup>Π and A<sup>2</sup>Σ<sup>+</sup> PECs of BNg (Ng = He–Xe) at the RCCSD(T)/AS $\zeta$  level dynamically corrected for BSSE.

**A. BNg, X<sup>2</sup>Π.** The following deductions can be made from Tables 2, 3, and 4. (a) All B–Ng interaction energies  $D_0$  are quite small as expected, the largest being about 210 cm<sup>−1</sup> (BXe), clearly pointing to the van der Waals character of the BNg molecules; see also the vBL Scheme (1). Observe as well that with the exception of BHe, bond distances  $r_0$  (BNg, Ng = Ne–Xe) remain more or less constant within ~0.1 Å (see Table 4). Corresponding  $D_0$  numbers of the A<sup>4</sup>Σ<sup>−</sup> state of BNg are naturally much larger: 227, 92, 1908, 3467, and ~6300 cm<sup>−1</sup> for Ng = He, Ne, Ar, Kr, and Xe, respectively.<sup>30</sup> (b) The dissociation energies  $D_0$  increase significantly from He (but see below) to Xe (see Table 4). As a matter of fact, they show excellent linear dependence as a function of the (experimental) static polarizabilities of Ng<sup>31</sup> (Figure 2). Extrapolating to the radioactive super heavy Ng radon (Rn;  $Z = 86$ ,  $\alpha = 5.3$  Å<sup>3</sup>), a good estimate of the  $D_0$  of BRn is obtained,  $D_0 \approx 280$  cm<sup>−1</sup>. (c) Electric dipole moments increase monotonically from  $\mu_e = 0.010$  (BHe) to 0.196 D (BXe) (Table 2). The  $\mu_e$  magnitude of BXe is about twice as large as the dipole moment of carbon monoxide, where  $\mu_e$  (CO; X<sup>1</sup>Σ<sup>+</sup>) = 0.122 D.<sup>32</sup> It is quite interesting that the  $\mu_e$  values display a perfect linear correlation with respect to the (experimental) polarizabilities  $\alpha$  of the Ng atoms (Ng = He–Xe) with a slope of  $d\mu/d\alpha = 0.048$  D/Å<sup>3</sup>. Thus, by extrapolating to the Rn atom as in (b),  $\mu_e$  (BRn)  $\approx$  0.26 D. (d) It is of interest at this place to say a few words on the spin–orbit (SO) splittings of the BNg systems. Relative to the interaction energies  $D_0$ , the SO effect is significant for the lightest molecules (BHe and BNe), and then its relative contribution fades away (see Tables 3 and 4). The SO interaction in the X<sup>2</sup>Π state gives two  $\Omega = \Lambda + \Sigma$  components,

**Table 5.** Total Energies,  $E$  ( $E_h$ ), Bond Lengths,  $r_{B-Ng}$  and  $r_{Ng-Ng}$  ( $\text{\AA}$ ), Angles,  $\angle NgBNg = \theta$  (deg), Atomization Energies,  $AE_e$  and  $AE_0$  ( $\text{cm}^{-1}$ ), Harmonic Frequencies,  $\omega_1(a_1)$ ,  $\omega_2(a_1)$ , and  $\omega_3(b_2)$  ( $\text{cm}^{-1}$ ), Dipole Moments,  $\mu_e$  (D), and Equilibrium BSSE/ $r_e$  Values ( $\text{cm}^{-1}$ ) of the  $\tilde{X}^2B_1$  State of  $BNg_2$ , Where  $Ng = He, Ne, Ar, Kr, \text{ and } Xe$  at the RCCSD(T)/AS $\zeta$  Level

Ng	$-E$	$r_{B-Ng}$	$r_{Ng-Ng}$	$\theta$	$+AE_e$	$+AE_0^a$	$\omega_1$	$\omega_2$	$\omega_3$	$\mu_e$	BSSE/ $r_e$
He	30.408 117	3.5484	2.9711	49.5	42.1	-5.1	27.7	28.7	38.1		1.49
Ne	282.321 69	3.4872	3.3839	58.1	94.4	52.0	14.6	29.6	40.5	0.041	12.61
Ar	1078.770 00	3.5586	3.9892	68.2	321.6	263.4	18.9	42.1	55.3	0.132	29.29
Kr	5529.163 36	3.6056	4.2691	72.6	442.8	384.6	12.4	45.3	58.5	0.191	22.18
Xe	681.602 60	3.6879	4.4306	73.8	639.3	576.9	19.6	47.1	58.1	0.285	20.84

$$^a AE_0 = AE_e - 1/2 \sum_{i=1}^3 \omega_i$$

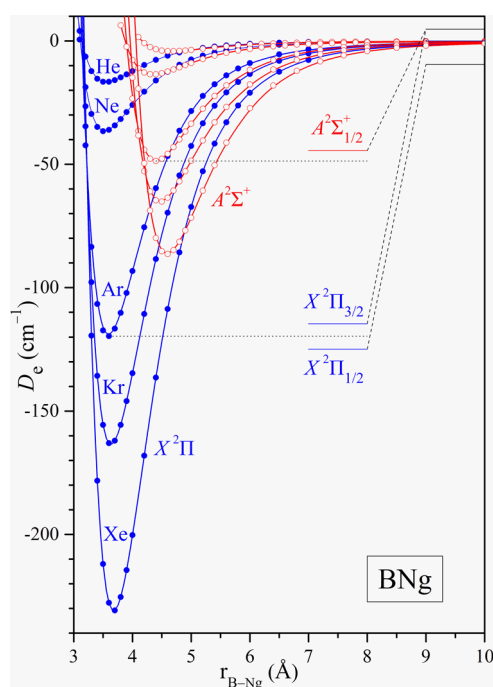


**Figure 1.** RCCSD(T)/AS $\zeta$ -BSSE corrected PEC's of the  $BNg$  diatomics,  $Ng = He-Xe$ . Blue  $\bullet$  and red  $\circ$  curves refer to the  $X^2\Pi$  and  $A^2\Sigma^+$  states. The shown SO splitting of  $BAr$  ( $X^2\Pi_{3/2}-X^2\Pi_{1/2}$ ) and the  $B$  ( $^2P_{3/2}-^2P_{1/2}$ ) +  $Ng$  ( $^1S$ ) asymptote are 10.32 and 14.34  $\text{cm}^{-1}$ , respectively.

1/2 and 3/2, the latter being the highest for all five  $BNg$  species (regular states). From Table 3, it can be seen that the 1/2–3/2 splitting ( $\Delta T$ ) of the  $BNg$  ( $Ng = He-Kr$ ) is practically constant within 0.7  $\text{cm}^{-1}$ ; the splitting increases by  $\sim 5$   $\text{cm}^{-1}$  in  $BXe$ . Notice as well the excellent agreement between experiment and theory in  $BAr$ , where  $\Delta T = 10.88 \pm 0.08^{29}$  versus 10.32  $\text{cm}^{-1}$ . Now taking into account the SO  $\Delta T$  values of the  $BNg$  and that of the  $B$  atom,  $\Delta T(^2P_{3/2} - ^2P_{1/2}) = 14.34$   $\text{cm}^{-1}$  (experimental value 15.287  $\text{cm}^{-1}$ ),<sup>4</sup> we obtain our final dissociation energies  $D_0$  (see Table 4). The  $X^2\Pi_{1/2}$  and  $X^2\Pi_{3/2}$  states correlate to the  $^2P_{1/2}$  and  $^2P_{3/2}$  atomic states of the  $B$  atom, respectively; corresponding interaction energies are referred to as  $D_0(1/2-1/2)$  and  $D_0(3/2-3/2)$ . Observe that with respect to the 1/2–1/2 components the  $BHe$  is unbound by 0.7  $\text{cm}^{-1}$ , but it is bound by 3.5  $\text{cm}^{-1}$  with respect to the 3/2–3/2 components. For the  $BNe$  molecule, the  $D_0(3/2-3/2)$  is about 4  $\text{cm}^{-1}$  larger than the  $D_0(1/2-1/2)$  value (see Table 4). The percentage influence in the  $D_0$  of the SO splittings diminishes drastically for the last three molecules  $BAr$ ,  $BKr$ , and  $BXe$ . (e) A word is needed as to the accuracy of our parameters, as compared to the existing experimental values for the  $X^2\Pi$

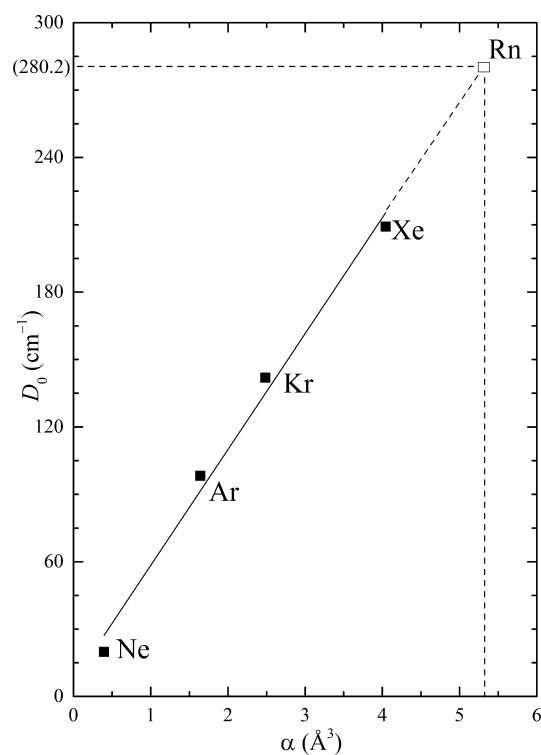


**Figure 2.** Extrapolation to  $Rn$  of the interaction energies  $D_0$  of  $BNg$  ( $X^2\Pi$ ),  $Ng = Ne-Xe$  versus the static experimental polarizabilities  $\alpha$  of  $Ng$ .

state. Assuming that the existing experimental values are correct, our largest discrepancy refers to the  $D_0(1/2-1/2)$  value of  $BKr$ ,  $159.4 \pm 1.2$  vs  $141.9$   $\text{cm}^{-1}$ , an error of about 10% (see Table 4). (f) Finally, the estimated number of vibrational levels of  $BNg$  are 1, 3, 5, 7, and 9 for  $Ng = He, Ne, Ar, Kr, \text{ and } Xe$ , respectively.

**B.  $BNg$ ,  $A^2\Sigma^+$ .** All our results on the  $A^2\Sigma^+$  states of the  $BNg$  diatomics are collected in the second part of Table 2; Figure 1 displays the RCCSD(T)/AS $\zeta$  BSSE corrected PECs. We are reminded that no other than BSSE corrections have been applied to the  $A^2\Sigma^+$  states. Our results, however, should be very reliable due to the smallness of core and scalar relativistic effects (vide supra). Notice also that no experimental results are available for this state, and also, there are no theoretical results for  $BHe$  and  $BNe$ . The quality of the limited theoretical values for the rest of the three species has been discussed in Introduction (see also Table 1).

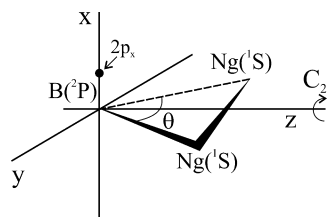
We comment briefly on some general features of the  $A^2\Sigma^+$   $BNg$  states. In accordance with symmetry, the  $A^2\Sigma^+$  states correlate to the  $^2P_{3/2}$  component of the  $B(^2P; M_L = 0)$  +  $Ng(^1S)$  atoms (see Scheme 2). The SO splittings raise the  $A^2\Sigma^+$

states of all BNg species by about  $4.5 \text{ cm}^{-1}$ , which is practically canceled due to the corresponding  $^2P_{3/2}$ - $^2P_{1/2}$  splitting of the B atom; the latter is  $\Delta T = 14.34 \text{ cm}^{-1}$  (Table 3), thus the  $^2P_{3/2}$  component raises by  $1/3\Delta T = 4.8 \text{ cm}^{-1}$  above the line of the weighted average, thus  $\Delta T(A^2\Sigma^+) - 1/3\Delta T(B) \approx 0$ . We observe that (a) energy separations  $T_0 = X^2\Pi - A^2\Sigma^+$ , as expected, are quite small, ranging from 17 (BNe) to  $133 \text{ cm}^{-1}$  (BXe). (b) The BHe molecule is unbound; the  $4.5 \text{ cm}^{-1}$  well depth cannot sustain a single vibrational level. (c) Bond distances are by  $\sim 1 \text{ \AA}$  larger and interaction energies ( $D_0$ ) about  $1/3$  of the corresponding  $X^2\Pi$  values (Tables 2 and 4). (d) The estimated number of vibrational levels of the BNg  $A^2\Sigma^+$  states are 2, 4, 5, and 5 for Ng = Ne, Ar, Kr, and Xe, respectively. The morphology of the PECs (Figure 1) makes the  $A^2\Sigma^+ - X^2\Pi$  transitions problematic due to unfavorable Franck–Condon factors.

**C. BNg<sub>2</sub>,  $\tilde{X}^2B_1$ .** All our numerical results on the symmetric triatomics BNg<sub>2</sub> (Ng = He–Xe) are given in Table 5 at the RCCSD(T)/A5 $\zeta$  level. We list geometries, atomization energies ( $AE$ ,  $AE_0$ ) with respect to B ( $^2P$ ) + 2Ng ( $^1S$ ), harmonic frequencies, dipole moments, and basis set superposition errors at equilibrium (BSSE/ $r_e$ ). No other corrections have been considered other than the BSSEs which, incidentally, are significant, even at the A5 $\zeta$  basis set level. No experimental data are available save certain observations on the existence of excited states of BNe<sub>2</sub><sup>33</sup> and BAr<sub>2</sub>.<sup>11,34</sup> On the theoretical side (nonab initio) calculations predict  $AE_0 = 53.19 \pm 0.3$  and  $295 \pm 0.21 \text{ cm}^{-1}$  for BNe<sub>2</sub><sup>33</sup> and BAr<sub>2</sub>,<sup>11,34</sup> respectively.

The following conclusions can be drawn going through the numerical results of Table 5: (a) The BHe<sub>2</sub> complex although it presents a surface depth of  $42 \text{ cm}^{-1}$  ( $AE_e$ ), it is unbound after including the harmonic ZPE correction. (b) All four BNg<sub>2</sub> complexes (Ng = Ne–Xe) are bent with the unique angle  $\theta$  of the isosceles triangle NgBNg increasing monotonically from  $58.1$  (BNe<sub>2</sub>) to  $73.8$  degrees (BXe<sub>2</sub>). Scheme 3 below gives a

Scheme 3



perspective geometrical representation of the BNg<sub>2</sub> molecules, suggesting as well an interaction between the two Ng atoms [see conclusion (c)]. The symmetry-defining electron distribution on the B atom is perpendicular to the molecular plane. When  $\theta = 60.0^\circ$ , the isosceles triangle becomes equilateral as, practically, in the case of the BNe<sub>2</sub> molecule ( $\theta = 58.1^\circ$ ). (c) The driving force of the acuteness of the angle  $\theta$ , more generally, the bend structure of the BNg<sub>2</sub> species, seems to be the attractive interaction of the two Ng atoms. Indeed at equilibrium, the in situ Ng–Ng bond lengths (Table 5) are very close to the RCCSD(T)/A5 $\zeta$  bond lengths of the free Ng<sub>2</sub> diatomics: 3.110, 3.787, 4.016, and 4.436 Å for Ne<sub>2</sub>, Ar<sub>2</sub>, Kr<sub>2</sub>, and Xe<sub>2</sub>, respectively. RCCSD(T)/A5 $\zeta$ -BSSE corrected interaction energies  $D_0$  of the free Ng<sub>2</sub> species are in relatively good agreement with the corresponding values given in ref 35 (experimental values in parentheses): 10.6 (16.3), 75.8 (84.8), 114.7 (126.6), and 163.5 (185.5)  $\text{cm}^{-1}$  for Ne<sub>2</sub>, Ar<sub>2</sub>, Kr<sub>2</sub>, and

Xe<sub>2</sub>, respectively. Now the barrier-to-linearity (BtL), BNg<sub>2</sub>( $\tilde{X}^2B_1; C_{2v}$ )  $\rightarrow$  NgBNg( $^2\Pi_u; D_{\infty h}$ ) at the RCCSD(T)/A5 $\zeta$  level including BSSE corrections, are BtL = 20.0, 75.9, 107.5, and  $162.9 \text{ cm}^{-1}$  for BNe<sub>2</sub>, BAr<sub>2</sub>, BKr<sub>2</sub>, and BXe<sub>2</sub>, respectively. The BtL numbers are smaller but very close to the interaction energies  $D_e = 25.8, 90.6, 125.8,$  and  $173.0 \text{ cm}^{-1}$  of the free Ng<sub>2</sub> diatomics, Ng = Ne, Ar, Kr, and Xe, respectively. The discussion above proves unequivocally that the BNg<sub>2</sub> complexes are absolutely floppy, their bent geometry being the result of the Ng–Ng in situ attractive interactions. From another perspective, the BNg<sub>2</sub> complexes can be thought as B( $^2P$ ) + Ng<sub>2</sub>( $^1\Sigma_g^+$ ) (see also Scheme 3). (d) In the light of the above, it is of no surprise that the atomization energies are in essence additive with respect to the BNg diatomics and the interactions of the free Ng<sub>2</sub> species at the same level of theory, that is,  $AE_0 \approx 2xD_0(\text{BNg}; X^2\Pi) + D_0(\text{Ng}_2; ^1\Sigma_g^+)$ . For instance, in the BAr<sub>2</sub> case, we obtain [see Table 2 and conclusion (c) above],  $2 \times 97.1 + 75.8 = 270.0 \text{ cm}^{-1}$  as contrasted to the calculated value of the BAr<sub>2</sub> (Table 5)  $AE_0 = 263.4 \text{ cm}^{-1}$ . Finally, the same holds true for the dipole moments, being practically equal to the vector sum of the dipole moments (“bond moments”) of the corresponding diatomic species, that is,  $\mu_e(\text{BNg}_2; \tilde{X}^2B_1) = (2 \times [\mu_e(\text{BNg}; X^2\Pi)]^2(1 + \cos \theta))^{1/2}$ . Indeed, through the vector sum we obtain [RCCSD(T) values in parentheses, Table 5],  $\mu_e(\text{BNg}_2; \tilde{X}^2B_1) = 0.038$  (0.041), 0.132 (0.132), 0.190 (0.191), and 0.313 (0.285) D for Ng = Ne, Ar, Kr, and Xe, respectively. Assuming a bond angle of  $\theta \approx 75^\circ$  for the BRn<sub>2</sub> complex (see the sequence of the  $\theta$  angles in Table 5) and using the estimated dipole moment of BRn,  $\mu_e \approx 0.26$  D, we get  $\mu_e(\text{BRn}_2) \approx 0.4$  D.

#### 4. SUMMARY

We present the first systematic and high level ab initio study on the electronic structure of the  $X^2\Pi$  and  $A^2\Sigma^+$  states of the BNg van der Waals diatomics and the  $\tilde{X}^2B_1$   $C_{2v}$  triatomics BNg<sub>2</sub>, Ng = He–Xe. With the exception of the spin–orbit interactions, which have been determined through the MRCI approach, the coupled-cluster single reference RCCSD(T) method was followed combined with quadruple to sextuple correlation consistent basis sets. For the  $X^2\Pi$  states in particular, a series of corrections have been taken into account, namely (dynamical) BSSE, SO splittings, core, and scalar relativistic effects and CBS limits. We report energetics, spectroscopic parameters, interaction energies, and electric dipole moments. Good estimates of  $D_0$  and  $\mu_e$  values are also given for the  $X^2\Pi$  state of the BRn system. Most of the results are reported for the first time, while the agreement with the existing experimental results is pretty good, considering the vdW nature of the BNg and BNg<sub>2</sub> complexes.

It is our belief that the comprehensiveness and the high calculational level of the present work resulting in practically definitive results, numerical or otherwise, will be useful to those interested in these van der Waals molecules.

#### ■ AUTHOR INFORMATION

##### Corresponding Author

\*E-mail: mavridis@chem.uoa.gr. Tel: +302107274501.

##### Notes

The authors declare no competing financial interest.

## REFERENCES

- (1) Kerkines, I. S. K.; Mavridis, A. Ab Initio Investigation of the LiHe  $X^2\Sigma^+$ ,  $A^2\Pi$ , and  $B^2\Sigma^+$  States: A Basis Set Study. *J. Phys. Chem. A* **2000**, *104*, 408–412.
- (2) Kerkines, I. S. K.; Mavridis, A. An Accurate Description of the LiNe  $X^2\Sigma^+$ ,  $A^2\Pi$ , and  $B^2\Sigma^+$  States. *J. Phys. Chem. A* **2001**, *105*, 1983–1987.
- (3) Kerkines, I. S. K.; Mavridis, A. Theoretical Investigation of the  $X^2\Sigma^+$ ,  $A^2\Pi$ , and  $B^2\Sigma^+$  States of LiAr and LiKr. *J. Chem. Phys.* **2002**, *116*, 9305–9314.
- (4) Kramida, A.; Ralchenko, Yu.; Reader, J. and NIST ASD Team. *NIST Atomic Spectra Database*, version 5.1 [Online]; National Institute of Standards and Technology: Gaithersburg, MD, 2013. <http://physics.nist.gov/asd> (accessed March 5, 2014).
- (5) Yang, X.; Hwang, E.; Dagdigian, P. J. Laser Fluorescence Excitation Spectroscopy of BNe Electronic States Correlating with the Excited Valence B(2s2p<sup>2</sup>D) Asymptote. *J. Chem. Phys.* **1996**, *104*, 599–606.
- (6) Yang, X.; Dagdigian, P. J. Fluorescence Excitation and Depletion Spectroscopy of the BAr Complex: Electronic States Correlating with the Excited Valence B(2s2p<sup>2</sup>D) Asymptote. *J. Chem. Phys.* **1997**, *106*, 6596–6606.
- (7) Hwang, E.; Huang, Y.-L.; Dagdigian, P. J.; Alexander, M. H. Experimental and Theoretical Characterization of the BAr van der Waals Complex: The  $X^2\Pi$ ,  $A^2\Sigma^+$  and  $B^2\Sigma^+$  Electronic States. *J. Chem. Phys.* **1993**, *98*, 8484–8495.
- (8) Yang, X.; Dagdigian, P. J. Spectroscopic Study of B–Kr Nonbonding Interactions. *J. Phys. Chem. A* **1997**, *101*, 3509–3513.
- (9) Yang, X.; Hwang, E.; Dagdigian, P. J.; Yang, M.; Alexander, M. H. Experimental and Theoretical Study of the B–Ne Nonbonding Interaction: The Free-Bound  $B^2\Sigma^+$ - $X^2\Pi$  Electronic Transition. *J. Chem. Phys.* **1995**, *103*, 2779–2786.
- (10) Kiljunen, T.; Eloranta, J.; Ahokas, J.; Kunttu, H. Optical Properties of Atomic Boron in Rare Gas Matrices: An Ultraviolet-Absorption/Laser Induced Fluorescence Study with Ab Initio and Diatomics-in-Molecules Molecular Dynamics Analysis. *J. Chem. Phys.* **2001**, *114*, 7157–7165.
- (11) Alexander, M. H.; Walton, A. R.; Yang, M.; Yang, X.; Hwang, E.; Dagdigian, P. J. A Collaborative Theoretical and Experimental Study of the Structure and Electronic Excitation Spectrum of the BAr and BAr<sub>2</sub> Complexes. *J. Chem. Phys.* **1997**, *106*, 6320–6331.
- (12) Dunning, T. H., Jr. Gaussian Basis Sets for Use in Correlated Molecular Calculations. I. The Atoms Boron through Neon and Hydrogen. *J. Chem. Phys.* **1989**, *90*, 1007–1023.
- (13) Feller, D. The Role of Databases in Support of Computational Chemistry Calculations. *J. Comput. Chem.* **1996**, *17*, 1571–1586.
- (14) Schuchardt, K. L.; Didier, B. T.; Elsethagen, T.; Sun, L.; Gurumoorathi, V.; Chase, J.; Li, J.; Windus, T. L. Basis Set Exchange: A Community Data Base for Computational Sciences. *J. Chem. Inf. Model.* **2007**, *47*, 1045–1052.
- (15) Peterson, K. A.; Figgen, D.; Goll, E.; Stoll, H.; Dolg, M. Systematically Convergent Basis Sets with Relativistic Pseudopotentials. II Small-Core Pseudopotentials and Correlation Consistent Basis Sets for the Post-d Group 16–18 Elements. *J. Chem. Phys.* **2003**, *119*, 11113–11123.
- (16) Raghavachari, K.; Trucks, G. W.; Pople, J. A.; Head-Gordon, M. A Fifth-Order Perturbation Comparison of Electron Correlation Theories. *Chem. Phys. Lett.* **1989**, *157*, 479–483.
- (17) Watts, J. D.; Gauss, J.; Bartlett, R. J. Coupled-Cluster Methods with Noniterative Triple Excitations for Restricted Open-Shell Hartree-Fock and Other General Single Determinant Reference Functions. Energies and Analytical Gradients. *J. Chem. Phys.* **1993**, *98*, 8718–8733.
- (18) Knowles, P. J.; Hampel, C.; Werner, H.-J. Coupled Cluster Theory for High Spin Open Shell Reference Wave Functions. *J. Chem. Phys.* **1993**, *99*, 5219–5227.
- (19) Douglas, M.; Kroll, N. M. Quantum Electrodynamical Corrections to the Fine Structure of Helium. *Ann. Phys.* **1974**, *82*, 89–155.
- (20) Hess, B. A. Applicability of the No-Pair Equation with Free-Particle Projection Operators to Atomic and Molecular Structure Calculations. *Phys. Rev. A* **1985**, *32*, 756–763.
- (21) Hess, B. A. Relativistic Electronic Structure Calculations Employing a Two-Component No-Pair Formalism with External-Field Projection Operators. *Phys. Rev. A* **1986**, *33*, 3742–3748.
- (22) de Jong, W. A.; Harrison, R. J.; Dixon, D. A. Parallel Douglas-Kroll Energy and Gradients in NWChem: Estimating Scalar Relativistic Effects Using Douglas-Kroll Contracted Basis Sets. *J. Chem. Phys.* **2001**, *114*, 48–53.
- (23) Jansen, H. B.; Ros, P. Non-Empirical Molecular Orbital Calculations on the Protonation of Carbon Monoxide. *Chem. Phys. Lett.* **1969**, *3*, 140–143.
- (24) Boys, S. F.; Bernardi, F. The Calculation of Small Molecular Interactions by the Differences of Separate Total Energies. Some Procedures with Reduced Errors. *Mol. Phys.* **1970**, *19*, 553–566.
- (25) van Duijneveldt, F. B.; van Duijneveldt-van de Rijdt, J. G. C. M.; van Lenthe, J. H. State of the Art in Counterpoise Theory. *Chem. Rev.* **1994**, *94*, 1873–1885.
- (26) Peterson, K. A.; Dunning, T. H., Jr. The CO molecule: The Role of the Basis Set and Correlation Treatment in the Calculation of Molecular Properties. *J. Mol. Struct.: THEOCHEM* **1997**, *400*, 93–117 and references therein.
- (27) Peterson, K. A.; Woon, D. E.; Dunning, T. H., Jr. Benchmark Calculations with Correlated Molecular Wave Functions. IV. The Classical Barrier Height of the  $H + H_2 \rightarrow H_2 + H$  Reaction. *J. Chem. Phys.* **1994**, *100*, 7410–7415.
- (28) Werner, H.-J.; Knowles, P. J.; Knizia, G.; Manby, F. R.; Schütz, M.; Celani, P.; Korona, T.; Lindh, R.; Mitrushenkov, A.; Rauhut, G. et al. *MOLPRO*, version 2012.1; 2012 (<http://www.molpro.net>).
- (29) Hwang, E.; Dagdigian, P. J. Spin-Orbit Splitting in the Ground  $X^2\Pi$  Electronic State of the BAr van der Waals Complex. *Chem. Phys. Lett.* **1995**, *233*, 483–488.
- (30) Papakondylis, A.; Miliordos, E.; Mavridis, A. Carbonyl Boron and Related Systems: An Ab Initio Study of B–X and YB≡BY ( $^1\Sigma_g^+$ ), where X = He, Ne, Ar, Kr, CO, CS, N<sub>2</sub> and Y = Ar, Kr, CO, CS, N<sub>2</sub>. *J. Phys. Chem. A* **2004**, *108*, 4335–4340.
- (31) *CRC Handbook of Chemistry and Physics*, 90th ed.; Lide, D. R., Ed.; 2009; pp 10–194.
- (32) Muentzer, J. S. Electric Dipole Moment of Carbon Monoxide. *J. Mol. Spectrosc.* **1975**, *55*, 490–491.
- (33) Tao, C.; Dagdigian, P. J.; Alexander, M. H. Experimental and Theoretical Investigation of the  $3s \leftarrow 2p$  Transition in the BNe<sub>2</sub> Complex. *Chem. Phys. Lett.* **2004**, *392*, 151–155.
- (34) Krumrine, J. R.; Alexander, M. H.; Yang, X.; Dagdigian, P. J. Experimental and Theoretical Study of the Electronic Spectrum of the BAr<sub>2</sub> Complex: Transition to the Excited Valence B(2s2p<sup>2</sup>D) State. *J. Chem. Phys.* **2000**, *112*, 5037–5043.
- (35) Huber, K. P.; Herzberg, G. *Molecular Spectra and Molecular Structure. IV. Constants of Diatomic Molecules*. Van Nostrand Reinhold Company: NY, 1979.